

Study on the Influence of Segmented Fuel Cell on Internal Parameter Distribution

Huicui Chen^{1*}, Wanchao Shan¹, Hongyang Liao¹, Tong Zhang¹, Pucheng Pei²

¹ School of Automotive Studies, Tongji University, Shanghai 201804, China

² State Key Laboratory of Automotive Safety and Energy, Tsinghua University, Beijing 100084, China

ABSTRACT

The nonuniform reaction inside the fuel cell seriously affects the performance and durability of the fuel cell. Segmented cell is a method of measuring the internal electrochemical reaction. A segment method which is easy to process is to groove on the terminal of the electrode plate. In order to study the influence of the grooving method on the segmented fuel cell, three-dimension, five serpent channels, single-phase fuel cell models with and without grooves on the anode plate are established in this paper. Under steady state, the polarization curve of the cell and the current density distribution of the anode terminal are compared. Under dynamic state, how the current density of the nine segments of the segmented cell changes with the cathode stoichiometric ratio is studied. The final conclusion has important guiding significance for the judgment of the internal reaction uniformity of the segmented fuel cell by grooving method and provide a theoretical basis for judging whether a fuel cell is out of oxygen by segmented fuel cell.

Keywords: PEMFC, Segmented Fuel Cell, Fluent, Grooves

1. INTRODUCTION

The improvement of the performance and durability of Proton Exchange Membrane Fuel Cell (PEMFC) is an important issue in fuel cell research[1]. Affected by operating parameters, geometric parameters and material properties, the electrochemical reaction in the active area of the membrane electrode inside the fuel cell is not uniform, which will affect the performance and durability of the fuel cell. In order to understand the distribution of the internal parameters of the fuel cell, the researchers developed segmented fuel cell[2].

The most commonly used segmented fuel cell designs can be divided into three categories: printed circuit boards (PCB), resistor networks and Hall effect sensor networks. Among them, PCB is the most widely

used because it is highly integrated, simple in structure, easy to process, install and debug. The main idea of PCB technology is to measure the internal parameters of the fuel cell by adding a printed circuit board with integrated test components to the fuel cell[2]. Through the analysis of the data collected in each segment, the distribution of current density and other parameters inside the fuel cell can be obtained, which can effectively reflect the internal situation of the fuel cell. The use of PCB technology for measurement in a segmented fuel cell was first proposed by S.J.C.Cleghorn[3], who used PCB as current collector plate and flow field, gold-plated the copper-clad area of the PCB and then processed the serpentine flow field into this board. This design structure is relatively compact and has been adopted by other teams so far[4-7]. However, the design and processing of this kind of PCB is complicated. Ibrahim Alaefour[8, 9] used a segmented bipolar plate and printed circuit board to form a segmented fuel cell, in which he grooved on the back of the bipolar plate to get sixteen isolated segments. Jiao[10] used the same method to measure the current density distribution during cold start. Among these studies, they mainly use segmented cells to measure the internal electrochemical reaction parameters of fuel cells, but there are few studies on the effect of segmented methods on fuel cells.

This paper mainly uses FLUENT to establish PEMFC three-dimensional, five serpent channels, single-phase models with and without grooves on the terminal of anode plate. Under steady conditions, by comparing their polarization curves and the difference in the current distribution of the anode terminal, the influence of the grooving method on the fuel cell performance is analyzed. Under dynamic conditions, by adjusting the cathode stoichiometric ratio, the fuel cell is gradually transformed from a severely air-deficient state to a state that air is excessive, and the response of the current density of each segment to the air supply is studied.

Selection and peer-review under responsibility of the scientific committee of CUE2020

Copyright © 2020 CUE

Studying the current distribution of the segmented cell's anode terminal and the dynamic response of different segments to the supply of air has important guiding significance for the determination of the internal reaction uniformity of the fuel cell and provide a theoretical basis for judging whether a fuel cell is out of oxygen by segmented fuel cell.

2. MODEL DEVELOPMENT

2.1 Model assumptions

In order to simplify the model, the following assumptions are set for the simulation[11, 12]:

- (1) The fuel cell temperature is constant
- (2) The reaction gas is ideal and incompressible
- (3) The water inside the fuel cell only exists in gaseous state, and the influence of liquid water is not considered
- (4) The gas diffusion layer, catalyst layer and membrane are homogeneous and isotropic porous media
- (5) The state of the gas in the flow channel is laminar flow

2.2 Governing equations of fuel cell

The complex reactions inside the fuel cell involve basic fluid dynamics equations, electrochemical reaction equations, gas diffusion equations, and water transfer equations, etc.

- (1) Conservation equations of mass, momentum, energy and composition

$$\frac{\partial(\varepsilon\rho)}{\partial t} + \nabla \cdot (\varepsilon\rho\vec{u}) = S_m \quad (1)$$

$$\frac{\partial(\varepsilon\rho\vec{u})}{\partial t} + \nabla \cdot (\varepsilon\rho\vec{u}\vec{u}) = -\varepsilon\nabla p + \nabla \cdot (\varepsilon\mu\nabla\vec{u}) + S_N \quad (2)$$

$$\frac{\partial(\varepsilon\rho c_p T)}{\partial t} + \nabla \cdot (\varepsilon\rho c_p \vec{u}T) = \nabla \cdot (k^{eff}\nabla T) + S_Q \quad (3)$$

$$\frac{\partial(\varepsilon c_k)}{\partial t} + \nabla \cdot (\varepsilon\vec{u}c_k) = \nabla \cdot (D_k^{eff}\nabla c_k) + S_k \quad (4)$$

- (2) Current conservation equation

$$\nabla \cdot (\sigma_e \nabla \Phi_e) + S_e = 0 \quad (5)$$

$$\nabla \cdot (\sigma_m \nabla \Phi_m) + S_m = 0 \quad (6)$$

- (3) Electrochemical reaction model

$$S_a = j_{a,ref} \left(\frac{C_{H_2}}{C_{H_2,ref}} \right)^{\gamma_a} \left(e^{\frac{\alpha_a F}{RT} \eta_a} - e^{-\frac{\alpha_c F}{RT} \eta_c} \right) \quad (7)$$

$$S_c = j_{c,ref} \left(\frac{C_{O_2}}{C_{O_2,ref}} \right)^{\gamma_c} \left(e^{\frac{\alpha_a F}{RT} \eta_a} - e^{-\frac{\alpha_c F}{RT} \eta_c} \right) \quad (8)$$

- (4) Open circuit voltage control equation

$$E = \frac{-\Delta G_0}{2F} + \frac{RT}{2F} \ln \left(\frac{P_{H_2} P_{O_2}^{0.5}}{P_{H_2O}} \right) \quad (9)$$

- (5) Consumption and production of substances in electrochemical reactions

$$\dot{m}_{H_2} = -\frac{M_{H_2} I_a}{2F} \quad \dot{m}_{O_2} = -\frac{M_{O_2} I_c}{4F} \quad \dot{m}_{H_2O} = -\frac{M_{H_2O} I_c}{2F} \quad (10)$$

2.3 Geometry and mesh

This paper uses gambit to establish a single fuel cell three-dimension model with five serpentine flow channels, which mainly includes the following nine parts: cathode and anode plates, flow channels, catalyst layers, gas diffusion layers and proton exchange membranes, as shown in the figure1. According to the literature[12], the flow field parameters and grid independence are studied, and the specific geometric parameters are finally determined, which is shown in table1.

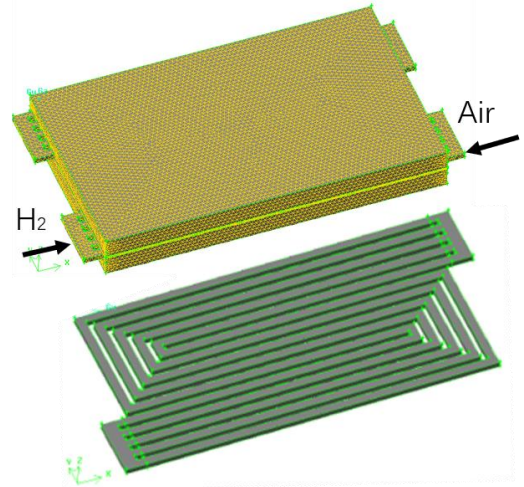


Fig 1 Geometry and mesh of model

Table 1. Geometric model dimensions of fuel cell.

Channel width	Channel height	Ridge width	Area of MEA
1.2mm	0.8 mm	0.8 mm	52mm×31.2mm
GDL height	Catalyst height	PEM height	Plate height
0.2mm	0.012mm	0.036mm	2mm

2.4 Material settings

In this paper, FLUENT is used to simulate the fuel cell model in first-order discrete format. The model parameters used are all based on the real properties of the material and are set in combination with literature[12, 13]. The specific parameter of the model is shown in Table 2.

Table 2. Parameters of the model

Plate	Density	Specific heat capacity	Thermal conductivity	Conductivity
	2719 kg·m ⁻³	871 J·kg ⁻¹ ·K ⁻¹	100 W·m ⁻¹ ·K ⁻¹	500 Ω ⁻¹ ·m ⁻¹
Gas diffusion layer	Density	Porosity	Conductivity	Viscous resistance
	2719 kg·m ⁻³	0.5	80 Ω ⁻¹ ·m ⁻¹	3.33×10 ¹² m ⁻²
Catalyst layer	Porosity	Viscous resistance	Surface-volume ratio	
	0.3	3.33×10 ¹² m ⁻²	200000 m ⁻¹	
Electrode	H ₂ diffusion coefficient	O ₂ diffusion coefficient	H ₂ O diffusion coefficient	Open circuit voltage
	9.15×10 ⁻⁵ m ² ·s ⁻¹	2.2×10 ⁻⁵ m ² ·s ⁻¹	2.56×10 ⁻⁵ m ² ·s ⁻¹	0.98 V
Proton exchange membrane	Thermal conductivity	Proton conductivity		
	2 W·m ⁻¹ ·K ⁻¹	1		

2.5 Model validation

In order to verify the accuracy of the model, this paper selects the experimental data in the literature[12] with the same flow field form and size for comparison, and uses the experimental conditions to set the boundary conditions of simulation, as shown in Table 3.

Table 3. Boundary conditions

Pressure	Temperature	Anode humidity
1.5 atm	343K	100%
Cathode humidity	Anode stoichiometry	Cathode stoichiometry
100%	1.5	2.5

The polarization curves obtained by the simulation and the experimental value are shown in the figure2(a). It can be seen that when the current density is less than 0.8 A/cm², the simulation model is consistent with the experimental results, but when the current density is greater than 0.8 A/cm², the simulation model and the experimental results are quite different. This is because this article assumes that water exists only in gaseous form, and does not consider the harsh conditions of flooding under high current density. Since this paper mainly studies the distribution of the current density of the segmented fuel cell and the dynamic response of each segment to cathode stoichiometric ratio, the generation of liquid water is not considered, so the model is considered to be reliable.

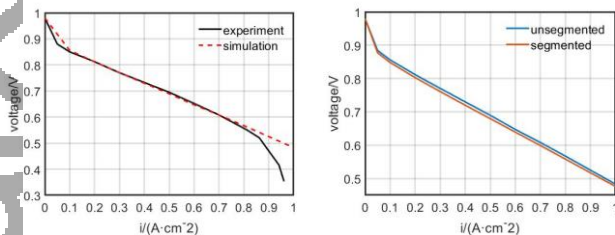


Fig 2 (a) Polarization curve of simulation and experimentation
(b) Polarization curve of segmented and unsegmented cell

3. RESULTS AND DISCUSSION

In order to study the influence of grooving on the anode plate on the fuel cell performance, on the basis of the existing model, the anode terminal was grooved with 1mm depth, 2mm wide in the direction parallel to the flow channel and 1.5mm wide in the direction perpendicular to the flow channel, and finally nine independent segments are obtained. These segments are numbered as shown in the figure3.

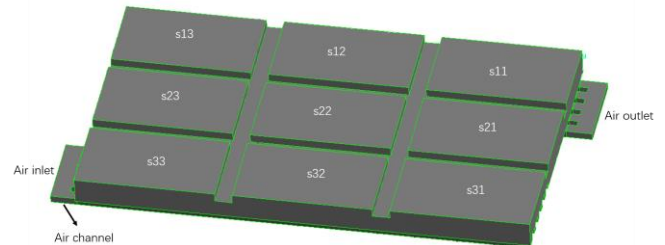


Fig 3 Segmented fuel cell and number of segment.

3.1 Steady conditions

3.1.1 Polarization curve

The polarization curve is the most important indicator for evaluating the performance of a fuel cell. The comparison of polarization curves between segmented cell and unsegmented cell is shown in the figure2(b). It can be seen from the figure that after being grooved, the performance of the cell drops slightly. Under the same current density, the voltage of the segmented cell is about 0.01V lower than that of the unsegmented cell. This is because the grooves break the structure of the fuel cell. However, this effect is relatively small, and it can be considered that the method of grooving on the anode plate to segment the fuel cell will not significantly damage the overall performance of the fuel cell.

3.1.2 Current density distribution

The current density of 0.7A/cm² is selected to study the current distribution of the segmented and unsegmented fuel cells. Under sufficient supply of reactants, the anode terminal current density of the

unsegmented cell is $0.7A/cm^2$, and that of the segmented cell is $0.839A/cm^2$. This is because in the fluent setting, the anode is grounded, and a current density of $0.7A/cm^2$ is applied to the cathode in the form of constant current. When the current is transmitted, due to the influence of the grooves, the current density at the anode terminal will increase. The specific current density distribution is shown in Figure4. Clearly, the anode terminal current density of unsegmented cell is consistent with the flow channel profile and is relatively uniform and that of the segmented cell is not uniform. Because the area of current transfer becomes smaller, there is a local increase in current density near the groove areas. This phenomenon is defined as “current concentration” in this paper and it can be seen in the figure4(b) that the “current concentration” phenomenon occurs near the grooving area, especially at the junction of two grooves.

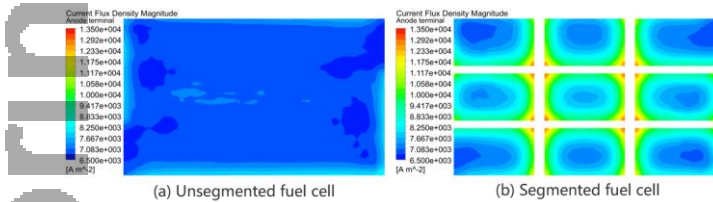


Fig 4 Current density distribution of anode terminal.

According to the current density of the nine segments, they can be divided into three types, as shown in the table4. In the first type, there are two “current concentration” phenomena, and s33 is at the air inlet zone, so its current density is the largest. Similarly, s11 and s13 are downstream of the air flow channel, so the current density is smaller, but the overall difference between the four segments of this type is not big. The second type of segment has three “current concentration” phenomena, the overall current density is larger than the first type. Similarly, the overall situation of the four segments is the same, and the current density of s12 which is in the downstream is slightly smaller. The third type of segment has four “current concentration” phenomena, so although it is not upstream of air flow channel, its current density is the largest.

This means that although grooving on the anode terminal has a small impact on the overall performance (polarization curve) of the fuel cell, it has a greater impact on the anode terminal current density distribution. Due to the existence of “current concentration” phenomena, there is a certain deviation between the current density distribution on the segmented fuel cell’s anode terminal and the uniformity of the internal electrochemical reaction, especially in the

middle segment (s22), which is most affected by “current concentration” phenomena.

3.2 Dynamic conditions

Although the measured current density of the segmented cell anode terminal is larger than the actual current density, the purpose of grooving is not to measure the terminal current density when the cell operates normally, but to reflect the nonuniformity of the internal electrochemical reaction through the current density of each segment when some bad circumstances happen. There are many reasons for the nonuniform internal reaction of the electrochemical reaction and the most common situation is starvation of reactant. Due to the fact that oxygen diffusion coefficient is small, and air is supplied instead of pure oxygen, the nonuniform electrochemical reaction inside the fuel cell caused by the starvation of oxygen on the cathode side is the most common.

This section simulates the cathode starvation situation, making the segmented fuel cell from a serious shortage of oxygen to a state that oxygen is excessive to research the dynamic response of each segment to the air supply. The specific operation is as follows: under the condition of the anode terminal grounded and the cathode terminal 0.6v constant voltage, write the UDF(User Defined Function) to set the cathode stoichiometric ratio as a function of time, the change of the cathode stoichiometric ratio and the response of segmented cell current density are shown in the figure5(a). As the cathode stoichiometric ratio steps up, the current density of the anode and cathode terminal also increases like waves, but due to the grooves on the anode plate and the “current concentration” phenomena, the increase magnitude of the anode terminal is larger. After 80s, the change rate of the anode and cathode terminal current density is less than 1%, which is close to stability. That means when the cathode stoichiometric ratio exceeds 1.6, increasing the air supply has almost no effect on the improvement of fuel cell performance.

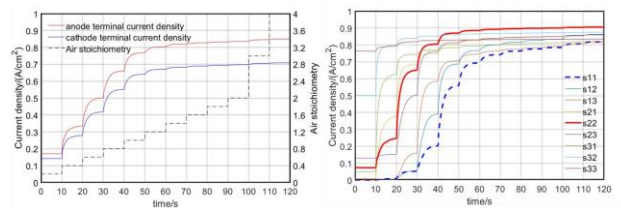


Fig 5(a)Current density of terminals&Air stoichiometry VS time (b)Current density of segments VS time

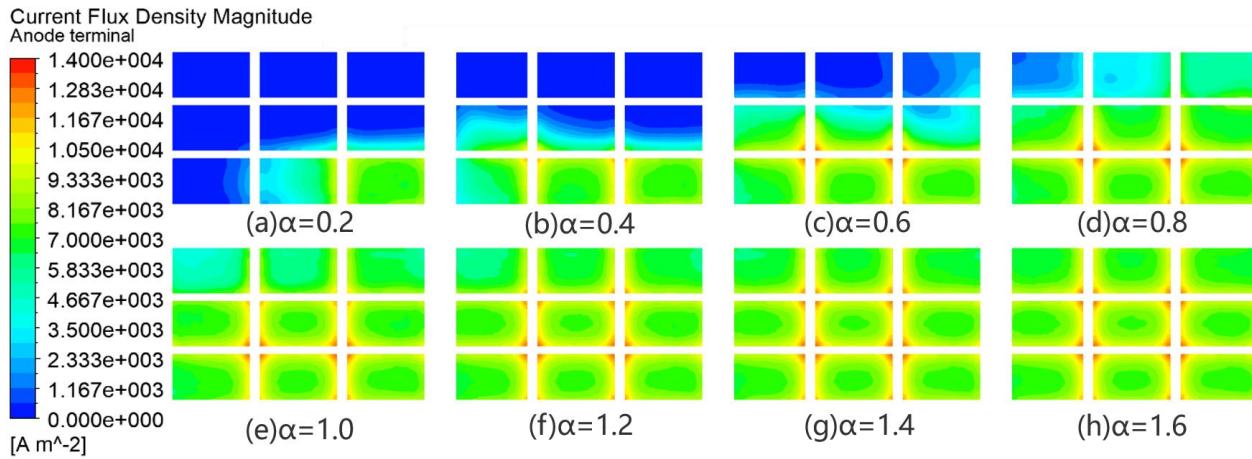


Fig 6 The changes of current density distribution with cathode stoichiometric.

Figure5(b) shows how the current density of the nine segments of the anode terminal changes with the increase of cathode stoichiometric ratio and figure6 shows the changes of current density distribution contours. Combine these two figures, it is clearly that with the gradual increase in the supply of air, the area where the electrochemical reaction occurs spreads along the direction of the air flow channel, and the current density of each segment increases with the trend similar to the current density change of the cathode and anode terminal in Figure5(a). Within 10-20s, due to the increase in air supply, the current density of the s31 and s21 segments, which are the first part to relieve oxygen starvation, has the largest increase. Similarly, with the increase step of the cathode stoichiometric ratio, the largest increase of the current density of each segment occurs when the channel corresponding to this segment relieves starvation for the first time. Due to the existence of “current concentration” phenomena, the current density of each segment does not decrease along the direction of the flow field, but like the steady-state situation, according to different types of segments, they are distributed in three current density intervals and s22 represented by the red line in figure5(b) is the largest. However, in practical applications, what we are most concerned about is s11 represented by the blue dashed line in figure5(b), because the starvation of oxygen usually occurs in the outlet area. The maximum increase time of s11 is 40s-50s, which corresponds to the situation that the cathode stoichiometric ratio changes from 0.8 to 1.0, but at this time, the current density of s11 is still significantly lower than other segments, which means cathode starvation at the outlet area. With the increase of cathode stoichiometric ratio, after 70s (when the cathode stoichiometric ratio is greater than 1.4), the

current density of s11 is almost the same as other three first-type segments, which means the internal electrochemical reaction of the fuel cell is almost uniform at this time. Therefore, it can be concluded that by comparing the current density of s11 and s13, which is also the first type of segment, it can be judged whether the fuel cell starts to experience oxygen starvation.

4. CONCLUSIONS

In this paper, three dimension, five-channel serpentine channels, single-phase PEMFC models with and without grooves on the anode plate are established to study the influence of grooving method on fuel cell performance.

In the steady-state model, the polarization curve and the current density contour of the anode terminal are compared and it is found that the grooves on the anode terminal has small impact on the overall performance of the fuel cell, but has greater impact on the current density distribution. The “current concentration” phenomenon is defined and according to it, and the nine segments are divided into three categories.

In the dynamic model, the trend of each segment changing with the cathode stoichiometry is studied, and the segment at the outlet of the air flow channel is analyzed. It is found that although the grooving method will affect the current density distribution of the anode terminal, the current density distribution difference between the segments can still accurately reflect the uniformity of the internal electrochemical reaction. The current density of the segment at the outlet can be compared with the same type of segment to determine whether the cathode is insufficient in oxygen supply.

ACKNOWLEDGEMENT

This research is sponsored by the Ministry of Science and Technology of China (No. 2018YFB0105405), the National Natural Science Foundation of China (21805210), the Shanghai Sailing Program (No. 18YF1424300), the Ministry of Science and Technology of China (No. 2017YFB0103102) and the Fundamental Research Funds for the Central Universities (No. 1700219153).

REFERENCE

- [1] Chen H, Zhao X, Zhang T, Pei P. The reactant starvation of the proton exchange membrane fuel cells for vehicular applications: A review. *Energy Conversion and Management*. 2019;182:282-98.
- [2] Pérez LC, Brand?o L, Sousa JM, Mendes A. Segmented polymer electrolyte membrane fuel cells—A review. *Renewable & Sustainable Energy Reviews*. 2011;15:169-85.
- [3] Cleghorn SJC, Derouin CR, Wilson MS, Gottesfeld S. A printed circuit board approach to measuring current distribution in a fuel cell. *Journal of Applied Electrochemistry*. 1998;28:663-72.
- [4] Gao J, Wen X, Xie G, Yang C, Fang H, Tang] H. In situ investigation of proton exchange membrane fuel cell performance with novel segmented cell design and a two-phase flow model. *Energy*. 2016.
- [5] Lin R, Weng Y, Li Y, Lin X, Xu S, Ma J. Internal behavior of segmented fuel cell during cold start. *International Journal of Hydrogen Energy*. 2014;39:16025-35.
- [6] Tang W, Lin R, Weng Y, Zhang J, Ma J. The effects of operating temperature on current density distribution and impedance spectroscopy by segmented fuel cell. *International Journal of Hydrogen Energy*. 2013;38:10985-91.
- [7] Lin R, Xiong F, Tang WC, Técher L, Zhang JM, Ma JX. Investigation of dynamic driving cycle effect on the degradation of proton exchange membrane fuel cell by segmented cell technology. *Journal of Power Sources*. 2014;260:150-8.
- [8] Alaefour I, Karimi G, Jiao K, Li X. Measurement of current distribution in a proton exchange membrane fuel cell with various flow arrangements – A parametric study. *Applied Energy*. 2012;93:80-9.
- [9] Alaefour I, Karimi G, Jiao K, Shakhshir SA, Li X. Experimental study on the effect of reactant flow arrangements on the current distribution in proton exchange membrane fuel cells. *Electrochimica Acta*. 2011;56:2591-8.
- [10] Jiao K, Alaefour IE, Karimi G, Li X. Simultaneous measurement of current and temperature distributions in a proton exchange membrane fuel cell during cold start processes. *Electrochimica Acta*. 2011;56:2967-82.
- [11] Alizadeh E, Rahimi-Esbo M, Rahgoshay SM, Saadat SHM, Khorshidian M. Numerical and experimental investigation of cascade type serpentine flow field of reactant gases for improving performance of PEM fuel cell. *International Journal of Hydrogen Energy*. 2017;42:14708-24.

[12] Iranzo A, Munoz M, Rosa F, Pino J. Numerical model for the performance prediction of a PEM fuel cell. Model results and experimental validation. *International Journal of Hydrogen Energy*. 2010;35:11533-50.

[13] Xinhai, Ben, Dong, Jun. CFD analysis of a novel modular manifold with multi-stage channels for uniform air distribution in a fuel cell stack. *Applied thermal engineering: Design, processes, equipment, economics*. 2017.